physical sciences forum

MDPI

Proceeding Paper

A New Representation of the 3C Model in the Quasi-Sturmian Approach to Ionization of Helium by Proton Impact †

Sergey Zaytsev [1,*], Lorenzo Ugo Ancarani [2], Darya Zaytseva [1], Alexander Zaytsev [1], Yury Popov [3,4] and Konstantin Kouzakov [5,6]

[1] Laboratory for Modeling of Quantum Processes, School of Fundamental and Computer Sciences, Pacific National University, Khabarovsk 680035, Russia; 2012002939@togudv.ru (D.Z.); 00001363@togudv.ru (A.Z.)
[2] Laboratoire de Physique et de Chimie Théoriques, Université de Lorraine, CNRS, 57000 Metz, France; ugo.ancarani@univ-lorraine.fr
[3] Skobeltsyn Institute of Nuclear Physics, Lomonosov Moscow State University, Moscow 119991, Russia; popov@srd.sinp.msu.ru
[4] Bogoliubov Laboratory of Theoretical Physics, Joint Institute for Nuclear Research, Dubna 141980, Russia
[5] Department of Nuclear Physics and Quantum Theory of Collisions, Faculty of Physics, Lomonosov Moscow State University, Moscow 119991, Russia; kouzakov@srd.sinp.msu.ru
[6] Branch of Lomonosov Moscow State University in Sarov, Sarov 607328, Russia
* Correspondence: 000282@togudv.ru
† Presented at the 1st International Online Conference on Atoms, 29–30 January 2026; Available online: https://sciforum.net/event/IOCAT2026.

Abstract

We investigate the 75 keV proton impact ionization of helium. The convoluted quasi-Sturmian approach is extended to treat both the direct ionization and the electron capture to the continuum by proposing an ansatz for the Coulomb three-body Green's function operator, for the kernel of which the leading asymptotic form contains the wave function of the 3C model. The resulting 3C-like model is tested numerically. Fully differential cross-sections are calculated for different energy-loss regimes and compared with recent experimental data.

Keywords: proton-impact ionization; electron capture to the continuum; 3C model

1. Introduction

Ion impact ionization of atoms is a fundamental phenomenon. For ionization of helium by 75 keV proton impact, detailed measurements of the fully differential cross-section (FDCS) have recently become available [1–4]. At high incident projectile energies, comparison of theoretical predictions with the experiment is satisfactory [5,6], but at intermediate energies the importance of electron capture to the continuum (ECC) increases, necessitating consideration of charge exchange channels alongside the direct ionization (DI) mechanism. While a number of theoretical approaches have been proposed in the literature, none provides a completely satisfactory description at ejected-electron velocities below, near, and above the projectile velocity, including the velocity-matching regime. Amongst them, only the CP method [7] and the WP-CCC method [8,9] (which use two-centered bases to obtain the total scattering wave function) are, in principle, able to deal with both ionization mechanisms. However, an ambiguity remains when combining the ECC and DI amplitudes to determine the ionization cross-section. In particular, there is no strict criterion that would allow one to choose between the 'coherent' cross-section, which is

Check for updates

Academic Editor: Omar Ariel Fojón

Published: 8 June 2026

Copyright: © 2026 by the authors. Licensee MDPI, Basel, Switzerland. This article is an open access article distributed under the terms and conditions of the Creative Commons Attribution (CC BY) license.

expressed through the sum of these amplitudes, and its 'incoherent' version, which is determined by the sum of the squares of the absolute values of the amplitudes.

We have recently developed an approach [10] based on parabolic convoluted quasi-Sturmian (CQS) functions. These basis functions are built using the Green's function operator associated with two model Hamiltonians (labeled 2C and IIC), each describing a pair of Coulomb interactions: the p^+-He^+ and e^--He^+ interactions for the 2C model, and the p^+-He^+ and p^+-e^- interactions for the IIC model. In both cases, the remaining interaction is treated via a Lippmann–Schwinger (LS) equation. It was found that the two model FDCS calculations were adequate for dealing with either the DI or the ECC mechanisms, according to the ejected electron energy value. The velocity-matching regime was further studied in detail within the IIC approach [11]. It appears that combining results from both methods is generally required to achieve an overall acceptable agreement.

In this paper, we propose to modify the model Green's function to account for all three pairwise Coulomb interactions; specifically, we supply the 2C Green's function with the Coulomb waves of the 3C model [12,13], yielding an unambiguous transition amplitude. In order to numerically test our parabolic Sturmian implementation, we first validate the method in its zero-order approximation by comparing calculated FDCSs with experimental measurements [1,4] across different energy-loss regimes. We also compare the present results with those obtained in [10], as to illustrate the benefit of the new approach.

Atomic units (a. u.) in which $\hbar = e = m_e = 1$ are used throughout unless otherwise specified.

2. Theory

Let us consider a proton (with mass $\boldsymbol{m_p}$) placed at position $\boldsymbol{R}$ and with momentum $\boldsymbol{K_0}$ impinging on a stationary helium target, supposed to be in its ground state and described by a wave function $\boldsymbol{\Phi^{(0)}(r, r')}$, where $\boldsymbol{r}$ and $\boldsymbol{r'}$ denote the coordinates of the two electrons. The proton is scattered with momentum $\boldsymbol{K}$, and an electron with momentum $\boldsymbol{k_e}$ is ejected from the target. The total energy $\boldsymbol{E = \frac{K^2}{2m_p} + \frac{k_e^2}{2}}$ is determined by the expression $\boldsymbol{E = \frac{K_0^2}{2m_p} + \mathcal{E}_{He} + \mathcal{E}_{He^+}}$, where $\boldsymbol{\mathcal{E}_{He} = -2.903724}$ a.u. and $\boldsymbol{\mathcal{E}_{He^+} = -2}$ a.u. In the frozen-core approximation, the final-state problem reduces to the motion of two charged particles—a proton and the ejected electron—in the Coulomb field of the residual He^+ ion left in the hydrogenic ground state (wave function $\boldsymbol{\psi_{1s}^{He^+}}$). Let $\boldsymbol{\hat{H}}$ denote the Hamiltonian of this three-body system $\boldsymbol{(e^-, He^+, p^+)}$. The transition amplitude can be obtained via the Green's function operator by solving the driven equation (see, e.g., [6])

$$\left[E - \hat{H}\right]|\Phi^{(+)} > = |\boldsymbol{K}_0, F >, \tag{1}$$

together with outgoing boundary condition; the driven term contains the projectile-target interactions

$$F(\boldsymbol{R}, \boldsymbol{r}) = < \psi_{1s}^{He^+} \left| \frac{2}{R} - \frac{1}{|\boldsymbol{R} - \boldsymbol{r}|} - \frac{1}{|\boldsymbol{R} - \boldsymbol{r}'|} \right| \Phi^{(0)} >, \tag{2}$$

where the matrix element is taken over the coordinate of the residual bound electron.

The scattering amplitude is given by

$$T_{\boldsymbol{K},\boldsymbol{k_e}} = < \Psi^{(-)}_{\boldsymbol{K},\boldsymbol{k_e}} | \boldsymbol{K}_0, F >, \tag{3}$$

where $\Psi^{(-)}_{\boldsymbol{K},\boldsymbol{k_e}}$ is the continuum state of the three-body Hamiltonian $\hat{H}$. Instead of the $\Psi^{(-)}_{\boldsymbol{K},\boldsymbol{k_e}}$ function, we propose to find the $\Phi^{(+)}$ function, since the asymptotic behavior of the latter determines the desired amplitude (3).

https://doi.org/10.3390/psf2026013010

To solve the driven Equation (1), we proposed in [10] to use parabolic convoluted quasi-Sturmian (CQS) functions constructed with one of the two model Hamiltonians, $\hat{H}_{2C}$ or $\hat{H}_{IIC}$, that include only two of the three Coulomb interactions. The remaining interaction is treated via a LS equation. Hereafter, we briefly recall the 2C model, and then introduce a more advanced model, labeled $3\widetilde{C}$ (more details are given in [14]).

2.1. The 2C Model

In this model, the continuum solution is the product $|\Psi_{\boldsymbol{K}}^{(-)}, \Psi_{\boldsymbol{k}_e}^{(-)}>$ where $\Psi_{\boldsymbol{K}}^{(-)}\left(\beta_p = \frac{m_p}{K}\right)$ and $\Psi_{\boldsymbol{k}_e}^{(-)}\left(\beta_e = -\frac{1}{k_e}\right)$ denote, respectively, the proton and electron Coulomb waves with the corresponding Sommerfeld parameter ($\beta_{1,2} = \frac{\mu_{1,2}Z_1Z_2}{k_{1,2}}$). The 2C product is the continuum solution of the separable Hamiltonian $\hat{H}_{2C}$ in the Jacobi coordinates ($\boldsymbol{R}$, $\boldsymbol{r}$) and implies that the operator $\hat{G}^{(+)}$ of the Coulomb three-body Green's function is approximated by $\hat{G}_2^{(+)} \equiv \left[E + i\varepsilon - \hat{H}_{2C}\right]^{-1}$. To calculate the ionization amplitude in the 2C model

$$T_{\boldsymbol{K},\boldsymbol{k}_e}^{(2C)} = \sqrt{2} < \Psi_{\boldsymbol{K}}^{(-)}, \Psi_{\boldsymbol{k}_e}^{(-)} | \boldsymbol{K}_0, F >, \tag{4}$$

(the factor $\sqrt{2}$ is related to the fact there are two identical target electrons) we use square-integrable Sturmians of parabolic coordinates [15], defined through Laguerre polynomials with a basis scale parameter. The size of the Sturmian basis representation is determined by the number of functions required to correctly describe the short-range term $|F\rangle$ on the right side of Equation (4) (the proton plane wave $|\boldsymbol{K}_0\rangle$ is considered separately). Note that the rate of convergence of the amplitude expansion can be improved by optimally choosing the scaling parameter of the basis set. Furthermore, for a fixed size of the total basis set, the number of proton basis functions can be significantly increased by reducing the number of functions of the electron coordinates. Indeed, due to the presence of the ground-state wave function of helium in $|F\rangle$, the number of electron basis functions can be kept relatively small. In this work, convergence was achieved by such an extension of the proton part of the basis set for the scaling parameter value used in [10]. The amplitude $T_{\boldsymbol{K},\boldsymbol{k}_e}^{(2C)}$ is expressed in terms of basis amplitudes, obtained by projecting Coulomb waves onto the Sturmian orthogonal complements. These basis amplitudes are expressible in closed form [6]. The remaining interaction (namely the proton–electron interaction) is treated via a LS equation, which we solve using for $\Phi^{(+)}$ an expansion on parabolic CQS functions constructed by applying the operator $\hat{G}_2^{(+)}$ onto the Sturmian orthogonal complements. The driven differential equation is subsequently transformed into a matrix equation. The 2C + LS approach leads to a scattering amplitude, noted $T_{\boldsymbol{K},\boldsymbol{k}_e}^{(2C+LS)}$.

2.2. The $3\widetilde{C}$ Model

In order to take into account the proton–electron interaction in a way similar to the 3C model continuum wave function [12,13], we consider the relative coordinate $\boldsymbol{r}_{ep} = \boldsymbol{r} - \boldsymbol{R}$, its conjugated momentum (which is codirected with the relative velocity between electron and proton) $\boldsymbol{k}_{ep} = \left(\frac{m_p}{m_p+1}\right)\boldsymbol{k}_e - \left(\frac{1}{m_p+1}\right)\boldsymbol{K}$, and the associated parabolic coordinate $\xi_{ep} \equiv r_{ep} + \hat{\boldsymbol{k}}_{ep} \cdot \boldsymbol{r}_{ep}$.

We then approximate the three-body Green's function operator $\hat{G}^{(+)}$ (whose explicit form is unknown) by modifying the Green's function operator of the 2C model as follows:

$$\hat{\tilde{G}}_3^{(+)} = |\mathcal{L} > \hat{G}_2^{(+)} < \mathcal{R}|, \tag{5}$$

so that the integral kernel $G_2^{(+)}(\boldsymbol{R}, \boldsymbol{r}; \boldsymbol{R}', \boldsymbol{r}')$ is complemented by the factors $\mathcal{L}(\xi_{ep})\mathcal{R}(\xi'_{ep})$:

$$\mathcal{L}(\xi_{ep}) = \mathcal{U}(\, i\beta_{ep},\, 1;\, -i\, k_{ep}\xi_{ep}\,), \tag{6}$$

$$\mathcal{R}(\xi_{ep}) = \Gamma(\, 1 - i\beta_{ep}\,)\mathcal{M}(\, i\beta_{ep},\, 1; -i\, k_{ep}\xi_{ep}\,), \tag{7}$$

where $\mathcal{U}$ and $\mathcal{M}$ are Kummer functions [16]; the Sommerfeld parameter is defined by $\beta_{ep} = -\frac{m_p}{(m_p+1)}\frac{1}{k_{ep}}$. Note that for a large hyperradius $\rho = \sqrt{m_p R^2 + r^2}$, the kernel $G_2^{(+)}(\boldsymbol{R}, \boldsymbol{r}; \boldsymbol{R}', \boldsymbol{r}')$ splits into two factors [17]. In particular, in this limit the factor, which depends on $\boldsymbol{R}$ and $\boldsymbol{r}$, takes the form of a six-dimensional outgoing spherical Coulomb wave. Thus, the left-hand factor $\mathcal{L}(\xi_{ep})$ allows us to equip the spherical wave with a phase factor corresponding to the proton–electron interaction. This is of particular importance when implementing the $3\widetilde{C}$ + LS approach. In turn, the right-hand factor $\mathcal{R}(\xi'_{ep})$ complements the part of the leading term of the kernel, which depends on $\boldsymbol{R}'$ and $\boldsymbol{r}'$, to the continuum wave function of the 3C model. Hence, from the resulting kernel asymptotic behavior, the $3\widetilde{C}$ model amplitude (up to a global phase factor that cancels in the FDCS) reads

$$T^{(3\widetilde{C})}_{\boldsymbol{K},\boldsymbol{k}_e} = \sqrt{2}\, e^{-\frac{\pi\beta_{ep}}{2}} < \Psi^{(-)}_{\boldsymbol{K}}, \Psi^{(-)}_{\boldsymbol{k}_e}, \mathcal{R} | \boldsymbol{K}_0, F >, \tag{8}$$

which strongly resembles the 3C model amplitude [12,13]. Here, the final-state bra is the 2C product state multiplied by the proton–electron Coulomb factor (7).

Like with the 2C model approach, the remaining interaction can be treated via a LS equation. The solution $\Phi^{(+)}$ is then proposed as an expansion on new CQS functions constructed by application of $\tilde{\tilde{G}}_3^{(+)}$; as above, the differential equation is then transformed into a matrix equation for the coefficients of such expansion. The present numerical results use the zero-order $3\widetilde{C}$ amplitude of Equation (8); the full $3\widetilde{C}$ + LS implementation will be reported in future work.

3. Results and Discussion

We calculated the FDCSs in the laboratory frame:

$$\frac{d^5\sigma}{dE_e d\Omega_e d\Omega_p} = k_e \frac{m_p^2}{(2\pi)^5}\frac{K}{K_0}|T_{\boldsymbol{K},\boldsymbol{k}_e}|^2 \tag{9}$$

with the ionization amplitudes $T^{(2C+LS)}_{\boldsymbol{K},\boldsymbol{k}_e}$ and $T^{(3\widetilde{C})}_{\boldsymbol{K},\boldsymbol{k}_e}$. Here, E_e and Ω_e are the ejected-electron energy and solid angle, while Ω_p denotes the scattered projectile solid angle. The kinematical and geometrical conditions are those selected in recent experiments performed with 75 keV proton impact [1,2,4]. In the ionization experiments under consideration, the energy of the ejected electron is determined by the energy loss of the projectile, namely,

$$E_e = E_{loss} - I,$$

where I = 24.59 eV is the ionization potential of the helium target. In Figure 1 we present results of calculations for electrons ejected into the scattering plane, for proton energy losses E_{loss} = 25.6 ($v_e \approx 0.037$ a.u.), 65.5 ($v_e \approx 1.73$ a.u.), and 85 eV ($v_e \approx 2.22$ a.u.), and for the scattering angle $\theta_p = 0.5$ mrad. The FDCS for E_{loss} = 30 eV ($v_e \approx 0.63$ a.u.) and $\theta_p = 0.43$ mrad is also calculated. Thus, in the considered energy regimes the velocities of the ejected electrons are respectively less than (cases (a) and (b)), nearly equal to (case (c)) and greater than (case (d)), the projectile velocity ($v_p \approx 1.73$ a.u.). In order to focus on the

benefits of the novel model, here we restrict the theoretical comparison with the 2C + LS results only.

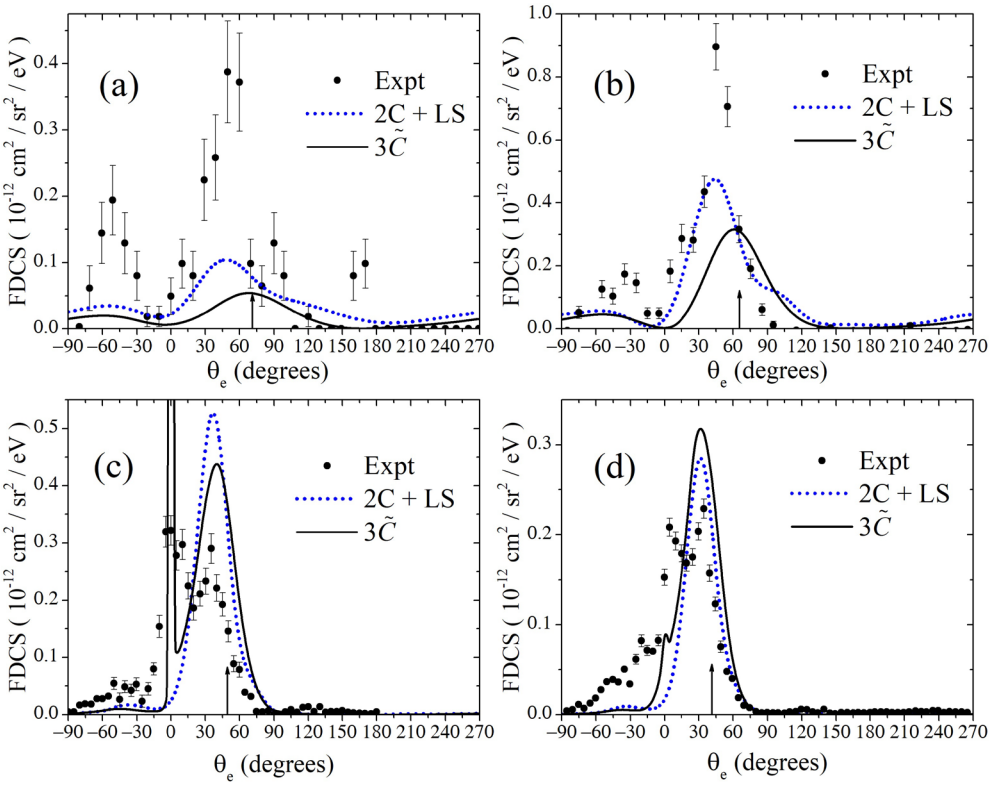


Figure 1. FDCSs for ionization of helium by 75 keV proton impact at different energy losses and proton scattering angles: (**a**) E_{loss} = 25.6 eV and θ_p = 0.5 mrad; (**b**) E_{loss} = 30 eV and θ_p = 0.43 mrad; (**c**) E_{loss} = 65.5 eV and θ_p = 0.5 mrad; (**d**) E_{loss} = 85 eV and θ_p = 0.5 mrad. The ionized electron is ejected at an angle θ_e in the scattering plane. Dotted line (blue)—2C+LS; thick solid line (black)—3$\widetilde{C}$ model. The FDCS curves are absolute calculations. Experimental data are from Ref. [4] for panel (**a**), and from Ref. [18], corrected in Ref. [9] for panel (**b**), and from Ref. [1] for panels (**c**,**d**). The arrow indicates the direction of the momentum transfer $\boldsymbol{q} = \boldsymbol{K}_0 - \boldsymbol{K}$.

At small energy losses the DI mechanism is dominant [9,10], and the 2C + LS approach should be able to describe the ionization process. As observed in Figure 1 (panels (a) and (b)), the 2C + LS approach (with an extended basis set) demonstrates both a binary peak and a recoil peak and is consistent with the experiment [4]; it is also consistent with the WP-CCC calculations [9]. The FDCS curves in Figure 1 are absolute calculations.

The FDCS obtained with our 3$\widetilde{C}$ model also exhibits a clear two-peak structure. For an energy loss of 25.6 eV, the recoil peak magnitude is approximately half that of the binary peak, in agreement with the experiment. However, the angular position of the binary peak in the 3$\widetilde{C}$ model is along the momentum transfer direction and thus differs from the measured one; this is possibly due to the limited validity of the 3$\widetilde{C}$ approximation at low electron energies. This can happen because the zero-order 3$\widetilde{C}$ model lacks the LS correction and the low-energy electron dynamics require a more complete basis treatment.

In the velocity-matching regime (Figure 1c), a pronounced forward peak due to electron capture to the continuum is observed experimentally. In a previous study [10], we have seen that the 2C model describes only the binary peak, while the IIC model reproduces the forward peak but underestimates the binary peak. We remind the reader that the forward peak is directed along the projectile velocity vector. In [11] we studied in detail how these two models pick up, separately, the DI and ECC mechanisms. By

spanning the energy loss around the velocity-matching value, we illustrated that the IIC model describes how the forward peak builds up (similarly to a 'resonance') in the electron–proton cusp region. As seen from the figure, the 2C + LS model calculation does not feature a forward peak. On the other hand, the $3\widetilde{C}$ model manages to yield results comparable to the experiment [1,4]. This is to be attributed to accounting also, from the outset, for the proton–electron Coulomb interaction. As the energy loss increases further (Figure 1d), the forward peak is still clearly present in the experiment while only a tiny peak is produced by the $3\widetilde{C}$ model (at best, a shoulder is seen in other theoretical approaches, like with the WP-CCC [9]). Here, we obviously have to exploit $3\widetilde{C}+$ LS calculations, as the first term is not enough.

In summary, 2C + LS captures the DI-related binary peak but not the ECC-related forward peak, IIC captures the ECC-related forward peak but underestimates the binary peak, and the $3\widetilde{C}$ model is intended to include both interactions in a single amplitude and therefore improves the velocity-matching case.

4. Conclusions

The comparison suggests that the proposed parabolic scheme, which incorporates all three pairwise Coulomb interactions at the level of the $3\widetilde{C}$ final-state ansatz, is applicable to the ionization problem in the energy regime considered. In the case when the contribution of the ECC mechanism is significant, the $3\widetilde{C}$ model is clearly superior. We plan, in a future investigation, to implement a $3\widetilde{C}$ + LS approach, in the hope that such a refinement will allow us to address the limitations of the $3\widetilde{C}$ model and thereby achieve improved agreement with the experiment.

Author Contributions: Conceptualization, S.Z., Y.P., L.U.A. and K.K.; methodology, S.Z., Y.P., L.U.A. and K.K.; software, A.Z., D.Z. and S.Z.; formal analysis, S.Z., Y.P., L.U.A. and K.K.; writing—original draft preparation, S.Z.; writing—review and editing, L.U.A., Y.P. and K.K. All authors have read and agreed to the published version of the manuscript.

Funding: This work is supported by the Ministry of Science and Higher Education of the Russian Federation (project no. FEME-2024-0005). The work of S.A.Z. was supported by the Russian Science Foundation under grant no. 24-22-20047, https://rscf.ru/en/project/24-22-20047/. Yu.V.P. and K.A.K. remark that this study was partially conducted under the state assignment of Lomonosov Moscow State University.

Institutional Review Board Statement: Not applicable.

Informed Consent Statement: Not applicable.

Data Availability Statement: The original contributions presented in this study are included in the article. Further inquiries can be directed to the corresponding author.

Acknowledgments: The research is carried out using the equipment of the Shared Facility Center "Data Center of FEB RAS" (Khabarovsk, Russia).

Conflicts of Interest: The authors declare no conflict of interest.

References

1. Dhital, M.; S. Bastola, S.; Silvus, A.; Lamichhane, B.R.; Ali, E.; Ciappina, M.F.; Lomsadze, R.; Hasan, A.; Madison, D.H.; Schulz, M. Target dependence of postcollision interaction effects on fully differential ionization cross sections. *Phys. Rev. A* **2019**, *100*, 032707. [CrossRef]
2. Dhital, M.; Bastola, S.; Silvus, A.; Davis, J.; Lamichhane, B.R.; Ali, E.; Ciappina, M.F.; Lomsadze, R.; Hasan, A.; Madison, D.H.; et al. Ejected-electron-energy and angular dependence of fully differential ionization cross sections in medium-velocity proton collisions with He and H_2. *Phys. Rev. A* **2020**, *102*, 032818.

3. Bastola, S.; Dhital, M.; Majumdar, S.; Hasan, A.; Lomsadze, R.; Davis, J.; Lamichhane, B.; Borbély, S.; Nagy, L.; Schulz, M. Interference effects in fully differential ionization cross sections near the velocity matching in p+He collisions. *Atoms* **2022**, *10*, 119. [CrossRef]
4. Majumdar, S.; Bastola, S.; Hasan, A.; Lomsadze, R.; Schulz, M. Separation of various higher-order effects in the ionization of helium by proton impact. *Phys. Rev. A* **2024**, *110*, 032814. [CrossRef]
5. Abdurakhmanov, I.B.; Kadyrov, A.S.; Alladustov, S.U.; Bray, I.; Bartschat, K. Fully differential cross sections for single ionization of helium by energetic protons. *Phys. Rev. A* **2019**, *100*, 062708. [CrossRef]
6. Zaytsev, A.S.; Zaytseva, D.S.; Zaytsev, S.A.; Ancarani, L.U.; Kouzakov, K.A. Parabolic quasi-Sturmian approach to proton-impact ionization of helium. *Phys. Rev. A* **2022**, *105*, 062818.
7. Walters, H.R.J.; Whelan, C.T. Differential ionization of a one-electron target under bare-ion impact: Application to proton-impact ionization of atomic hydrogen. *Phys. Rev. A* **2015**, *92*, 062712.
8. Abdurakhmanov, I.B.; Bailey, J.J.; Kadyrov, A.S.; Bray, I. Wave-packet continuum-discretization approach to ion-atom collisions including rearrangement: Application to differential ionization in proton-hydrogen scattering. *Phys. Rev. A* **2018**, *97*, 032707. [CrossRef]
9. Spicer, K.H.; Antonio, N.W.; Schöffler, M.S.; Schulz, M.; Kadyrov, A.S. Coupled-channel calculations of fully differential cross sections. *Phys. Rev. A* **2025**, *112*, 032806. [CrossRef]
10. Zaytsev, S.A.; Zaytseva, D.S.; Zaytsev, A.S.; Ancarani, L.U.; Kouzakov, K.A.; Popov, Y.V. Quasi-Sturmian basis set for problems of single ionization of helium by proton impact with rearrangement. *Phys. Rev. A* **2025**, *111*, 052812. [CrossRef]
11. Popov, Y.V.; Zaytsev, S.A.; Kouzakov, K.A.; Ancarani, L.U. Single Ionization of Helium Atom by 75 keV Protons Near the Cusp Region. In *Reviews of Light and Heavy Particle Collisions with Atoms and Molecules*; Belkić, Ď., Ed.; World Scientific: Singapore, 2026; pp. 207–226.
12. Garibotti, C.R.; Miraglia, J.E. Ionization and electron capture to the continuum in the H^+-hydrogen-atom collision. *Phys. Rev. A* **1980**, *21*, 572. [CrossRef]
13. Brauner, M.; Briggs, J.S.; Klar, H. Triply-differential cross sections for ionisation of hydrogen atoms by electrons and positrons. *J. Phys. B* **1989**, *21*, 2265. [CrossRef]
14. Zaytsev, S.A.; Zaytseva, D.S.; Zaytsev, A.S.; Ancarani, L.U.; Kouzakov, K.A.; Popov, Y.V. Ionization of helium by proton impact in a quasi-Sturmian approach built upon the 3C model. *Atoms* **2026**, *14*, 36. [CrossRef]
15. Zaytsev, S.A.; Ancarani, L.U.; Zaytsev, A.S.; Kouzakov, K.A. A parabolic quasi-Sturmian approach to quantum scattering by a Coulomb-like potential. *Eur. Phys. J. Plus* **2020**, *135*, 655. [CrossRef]
16. Buchholz, H. *The Confluent Hypergeometric Function*; Springer: Berlin/Heidelberg, Germany, 1969.
17. Merkuriev, S.P.; Faddeev, L.D. *Quantum Scattering Theory for Several Particle Systems*, 1st ed.; Springer: Dordrecht, The Netherlands, 1993.
18. Schulz, M.; Hasan, A.; Maydanyuk, N.V.; Foster, M.; Tooke, B.; Madison, D.H. Kinematically complete experiment on single ionization in 75-keV p + He collisions. *Phys. Rev. A* **2006**, *73*, 062704. [CrossRef]

Disclaimer/Publisher's Note: The statements, opinions and data contained in all publications are solely those of the individual author(s) and contributor(s) and not of MDPI and/or the editor(s). MDPI and/or the editor(s) disclaim responsibility for any injury to people or property resulting from any ideas, methods, instructions or products referred to in the content.